Journal of Pharmaceutical Research International

33(44A): 244-264, 2021; Article no.JPRI.73066
ISSN: 2456-9119
(Past name: British Journal of Pharmaceutical Research, Past ISSN: 2231-2919, NLM ID: 101631759)

Antimicrobial and Hepatoprotective Effect of Chitosan Nanoparticles : *In-vitro* and *In-vivo* Study

Hanaa A. El-Shafei[1*], Gihan F. Asaad[2], Yomna A. M. Elkhateeb[1], Walaa A. El-Dakroury[3], Hoda A. Hamed[1], Azza Hassan[4] and Yousra A. Nomier[5]

[1]Microbial Chemistry Department, Genetic Engineering Division, National Research Centre (ID: 60014618), Dokki, Giza, Egypt.
[2]Pharmacology Department, Medical Division, National Research Centre (ID: 60014618), Dokki, Giza, Egypt.
[3]Department of Pharmaceutics and Pharmaceutical Technology, Faculty of Pharmacy, Badr University in Cairo (BUC), Egypt.
[4]Department of Pathology, Faculty of Veterinary Medicine, Cairo University, Giza, Egypt.
[5]Phamacology and Toxicology Department, Pharmacy College, Jazan University, Saudi Arabia.

Authors' contributions

This work was carried out in collaboration among all authors. All authors read and approved the final manuscript.

Article Information

DOI: 10.9734/JPRI/2021/v33i44A32613
Editor(s):
(1) Lesław Juszczak, University of Agriculture, Poland.
(2) Dr. Rafik Karaman, Al-Quds University, Israel.
Reviewers:
(1) Divya Deodhar, India.
(2) Anita Tahlan, India.
(3) Pallav Kaushik Deshpande, Barkatullah University, India.
Complete Peer review History: https://www.sdiarticle4.com/review-history/73066

Original Research Article

Received 03 July 2021
Accepted 13 September 2021
Published 18 September 2021

ABSTRACT

Nanotechnology has become an extensive area of study due to the peculiar properties of nanoparticles. Chitosan is considered the most promising material for future applications. The purpose of this study was to highlight the antimicrobial and hepatoprotective properties of Chitosan nanoparticles (CTS), as well as their efficacy against multidrug-resistant pathogens and various applications as a natural antioxidant in the biomedical field. CTS were prepared with or without surfactant (L-α-lecithin, Tween 80) based on inotropic gelation of chitosan with sodium alginate. The nanoparticle obtained displayed a spherical shape with a particle size ranging from 54.3±20.8 to 1256±16.8 nm, zeta potential ranging from 24±1.2 to 30.8±1.1 mV, and polydispersity index

**Corresponding author: E-mail: Prof_elshafie@hotmail.com;*

ranging from 0.274±0.09 to 0.553±0.06. Minimum inhibitory concentration (MIC) and minimum bactericidal concentration (MBC) calculations were used to evaluate the antibacterial activity of CTS against four human pathogens: *Bacillus subtilis* ATCC6633, *Staphylococcus aureus* NRRLB-767, *Escherichia coli* ATCC25955, and *Pseudomonas aeruginosa* ATCC101455. The MIC values were 156.3, 39.4, 78.1, and 78.1 ug/mL, while the MBC values were 500,156.3, 312.5, and 312.5 ug/mL, respectively. *S.aureus* was the most susceptible, while *B. subtilis* was the most resistant. The hepatoprotective effect was determined by measuring antioxidant, antiapoptotic, and inflammatory biomarkers, histopathological and immunohistochemical studies. Hepatoprotective results showed a remarkable ameliorative effect against hepatotoxicity induced by CCl_4.

Keywords: Chitosan nanoparticles (CTS); antimicrobial activity; pathogenic microorganisms; hepatoprotective effect; histopathology; immunohistochemical studies.

1. INTRODUCTION

Chitosan discovered by Rouget [1] is the world's second most abundant natural polymer after cellulose, mainly composed of 1,4- β-linked residues of glucosamine and N-acetyl-glucosamine. The primary source of commercial chitosan is substantial deacetylation of the parent polymer chitin, which is found in green algae, Zygomycetes class fungus cell walls, crustacean exoskeleton [2], Panarthropoda cuticle (Arthropoda, Onychophora, Tardigrada) [3], and *Plumatella repens* (Bryozoa) [4].

Chitosan is regarded as one of the most promising materials for future applications due to its unique macromolecular structure, biocompatibility, biodegradability, and other intrinsic functional properties such as physicochemical, antimicrobial, and biological qualities, as well as its bioactivity that is safe for humans [5]. Over the last two decades, chitosan has gotten a lot of interest in disciplines like dentistry, ophthalmology, biomedicine, and biotechnology [5,6]. In 2017 Chitosan has been approved as GRAS (General Recognized as Safe) by US-FDA and EU for dietary use and medical uses such as bandages and drug encapsulation.

Scientific evidence has recently become useful in supporting the concept of micro/ nanocarriers, particularly nanoparticles and nanofibers [7]. Nanoparticles have unique properties when compared to their bulk counterparts because of their atomic-scale reduction [8]. In biotechnical applications, chitosan nanofiber can be generated from the fly *Drosophila melanogaster* via electrospinning synthesis [9].

The characteristics of materials alter at the nanoscale. This is because bulk materials have generally consistent properties regardless of their size, but as the size lowers the percentage of surface atoms increases in comparison to the bulk content. This enables nanoparticles to have a wide range of properties [10]. Nanomaterial has recently developed as the most promising therapeutic remedy for infectious microbes that are resistant to conventional therapies. Antibiotic drugs are no longer effective against microbes that have developed resistance to them, so nanomaterials have emerged to address these growing microbe infection-related issues. In the 1990s, publications documenting the antimicrobial capacity of chitosan and its derivatives, which exhibit a broad range of activities for human pathogens and food-borne species, heralded the new age of chitosan research [11-14]. Chitosan and its derivatives' range of antimicrobial activity extend to include filamentous fungi, yeasts, and bacteria, being more active against Gram-positive than Gram-negative bacteria [1,15].

The antimicrobial mode of action is affected by many factors, including intrinsic, environmental, microbe, and physical state affecting chitosan-mediated inhibition [16]. Chitosan's most common proposed antibacterial function is by binding to the negatively charged bacterial cell wall that causes cell disruption, thus altering the permeability of the membrane, followed by attachment to DNA that causes DNA replication inhibition and subsequently cell death [17].

An *in vivo* study was conducted to scout the protective effect of chitosan against carbon tetrachloride CTS.

Carbon tetrachloride (CCl_4) is a standard xenobiotic that can induce acute and chronic liver toxicity in a time and dose manner. Inside the body, CCl_4 is metabolized through cytochrome P450 in the liver endoplasmic reticulum to trichloromethyl and trichloromethyl peroxyl

radicals which are considered as critical forms for the devastating effects of CCl_4 [18]. In parallel with oxidative stress, CCl_4 can also alleviate liver inflammation which is mediated by pro-inflammatory cytokines, tumor necrosis factor (TNF-α), and interleukin -1β (IL-1β) [19]. The nuclear factor Kappa B (NF-κβ) which is induced because of oxidative stress is the most abundant factor controlling the body immune response to external xenobiotics and thus the expression of cytokines is regulated by NF-κβ. This makes it very interesting for researchers to find drugs targeting NF-κβ as a promising approach for the treatment of liver inflammations.

The goal of this study was to create Chitosan nanoparticles, characterize their physicochemical properties, and assess their antimicrobial activity to combat the era of multi-drug resistance in pathogenic medical organisms, as well as to assess biomedical parameters in liver tissue and the potential protective role of chitosan nanoparticles (CTS) in regulating CCl_4 induced by rat hepatotoxicity.

2. MATERIALS AND METHODS

2.1 Material

Chitosan medium molecular weight, deacetylation degree 75-85 % were purchased from Sigma Aldrich Chemical Co. (St. Louis, MO, USA), Sodium alginate was purchased from Himedia company (Mumbai, India). L-α-lecithin (Acros organics, USA). Carbon tetrachloride purchased from Sigma, St. Louis – USA, other chemicals were of analytical grades. Luria-Bertani agar medium (LB) was purchased from Merck, Germany. Muller Hinton Agar was purchased from Difco Laboratories Detroit Michigan USA.

2.2 Microorganisms

Four different human pathogens two Gram-positive bacteria, *Bacillus subtilis* ATCC6633, *Staphylococcus aureus* NRRLB767, and two Gram-negative bacteria, *Escherichia coli* ATCC 25955, *Pseudomonas aeruginosa* ATCC101455 were obtained from the University of AL-Azhar, Faculty of Medicine, Cairo, Egypt, and used for in vitro chitosan nanoparticles antimicrobial activity testing. *Bacillus subtilis*, a Gram-positive bacterium found in the soil and the gastrointestinal tract of ruminants and humans. It was chosen because of the enhanced resistance of Gram-positive bacteria to the bactericidal action of chitosan compared to Gram-negative bacteria, except for *E. Coli. Staphylococcus aureus*, a Gram-positive bacterium that is a common cause of skin infections, respiratory infections, and food poisoning, is an opportunistic pathogen. It is also one of the five most common causes of infections acquired from the hospital. *Escherichia coli* is a Gram-negative bacterium and, based on its infectious characteristics, has been selected in comparison to other genera. *Pseudomonas aeruginosa* is a multidrug-resistant Gram-negative pathogen associated with severe diseases such as ventilator-associated pneumonia and multiple sepsis syndromes, which are hospital-acquired infections.

2.3 Methods

2.3.1 Preparation of chitosan nanoparticles (CTS)

Three separate reported methods [20-22] (with a minor modification) were used to prepare CTS. Briefly, In the first method, chitosan was dissolved in 1 % acetic acid. L-α-lecithin solution was prepared by dissolving in absolute ethyl alcohol to prepare 50 mg/mL solution at room temperature. The nanoparticle suspension was prepared while stirring at 1000 rpm by dripping of L-α-lecithin solution into the chitosan solution. To prepare a 10 mg/mL solution. The prepared solution was dripped into 10 mg/mL alginate solution in ratio 6:4. The second and third formulations were prepared by ionotropic gelation of sodium alginate as a core and then polyelectrolyte complexation with chitosan with or without surfactant. In short, 12 mg/mL chitosan solution was prepared by dissolving in 2% acetic acid and the pH of the solution was changed to 4.8 using 1N HCL and 1N NaOH. The chitosan solution was splinted into two parts, adding 0.3% Tween 80 to the first part under continuous stirring for 2 h at 60°C to create a homogeneous solution. By dissolving sodium alginate in distilled water at a concentration of 6 mg/mL, an alginate solution was prepared and the pH was adjusted to 5.2. The alginate solution was kept overnight at room temperature. The chitosan solutions were dripped into the alginate solution under stirring at 1000 rpm in both formulations. Using a probe sonicator (Branson, Sonifier 250, Mexico) the three formulations were homogenized for 15 min at 20 kHz frequency, to minimize the particle size. The final concentration of chitosan was 6mg/ml in the three formulations

2.4 Methods of Analysis

2.4.1 Characterization of chitosan nanoparticles (CTS)

Particle size (mean diameter), size distribution (polydispersity index, PDI), and zeta potential were assessed for the freshly prepared nanoparticle suspensions through dynamic light scattering using (Zetasizer Nano ZS, Malvern Instruments, Worcestershire, UK). The morphology of nanoparticles was estimated by an optical microscope (Olympus, Germany) fitted with an ocular reticulum and connected to a computer-connected polaroid camera through Am scope software v4.8.15934. All of the measurements were performed in triplicate.

2.5 Microbiological Studies

2.5.1 Activation of microorganisms

Luria-Bertani medium (LB) is a semi-synthetic medium used for all indicators for general cultivation. All cultures were incubated at 37 ° C and were all activated by incubation for 24 hours.

2.5.2 Determination of the antibacterial activity of CTS

The agar well diffusion method was used as described by Catchpole [23]. The Mueller-Hinton agar plates were heavily seeded with a 0.1 mL broth culture of the test species. Wells 6 mm in diameter were punched with a sterile cork drill over the agar plates. The floors of the wells were formed in the broken wells by casting 50-100 µL of molten muller-Hinton. CTS solution was applied to various wells in the plate with a micropipette. These plates were then held for exactly 3 hours at a low temperature (4 °C) to allow diffusion of the substances and then incubated for 24 hours at 37 ° C. Absence or presence of inhibition zones as well as their diameters, were recorded.

2.5.3 Determination of chitosan nanoparticles (CTS) MIC and MBC on the pathogenic bacteria

The broth dilution method [24] used *Bacillus subtilis, Staphylococcus aureus, Escherichia coli,* and *Pseudomonas aeruginosa* as indicator species to assess the MIC and MBC values of nano-chitosan:

a) Different CTS concentrations, previously prepared at serial two-fold concentrations, were placed in LB broth medium tubes for this process.
b) One ml of pathogenic organism inoculum (2×10^5 CFU/m L) was applied separately to tubes containing CTS growth media in serial two-fold dilution (4.9, 9.8, 19.7, 39.4, 78.1, 156.3, 312.5, 625 ug/mL broth medium). The control tube was CTS-free.
c) Turbidity tubes were analyzed after 24 hours as a growth indicator. The lowest CTS concentration that inhibits the growth of the organism, as detected by lack of visual turbidity, is considered the minimum inhibitory concentration (MIC) compared to control.
d) The MBC (minimum bactericidal concentration) was defined as the lowest concentration of test compounds that did prevent any visible bacterial growth on LB agar plate after 24 h incubation at 37 °C. MBC was determined by assaying the live microorganisms in those tubes from the MIC test that showed no growth. A loop full of each of those tubes was inoculated on LB agar and examined for growth signs. Bacteria growth indicates the presence of these bacteria in the initial tube. On the contrary, the initial tube did not contain any living bacteria [25].

2.6 Pharmacological Studies

2.6.1 Animals

Forty male Wistar rats (250-350 g) were purchased from the animal breeding unit at the National Research Centre -Dokki- Giza – Egypt. Animals were housed in cages with water and food ad libitum, and the animal room temperature was kept at a constant temperature of 20 ± 1°C on a 12-hour light/12-hour dark cycle. Adequate measures were taken to minimize the pain or discomfort of the animals.

2.6.2 Experimental protocol

Forty rats were divided randomly into four groups; Group 1: is kept as control negative (n = 10), Group 2, 3, and 4 were injected intraperitoneally with carbon tetrachloride (CCl_4) in a dose of 1.5 mg/kg dissolved in paraffin oil (1:1 w/v) twice a week for 2 weeks [26]. Group 3: administered CTS 10mg/kg daily for 15 days concurrently with CCl_4. Group 4: administered CTS 20mg/kg daily for 15 days concurrently with CCl_4. 48 hours after the end of the experiment, blood samples were taken from the retro-orbital

plexus under a low dose of ketamine anesthesia for estimation of liver function test in serum (AST and ALP). Animals were sacrificed by cervical dislocation under anesthesia and livers from all rats were extracted and divided into two parts. One part is kept in -80° C for determination of malondialdehyde (MDA), reduced glutathione (GSH), catalase (CAT), superoxide dismutase (SOD), caspase-3 (Casp-3), tumor necrosis factor (TNF-α), and IL-1β using ELISA kits (TNF-α; Biolegend Inc®, USA), interleukin-1β (IL-1β; Cohesion Biosciences, UK) and following the instruction of the manufacturer. The other part was kept in formalin 10% for histopathological examination and immunohistochemical studies.

2.6.3 Determination of serum biochemical parameters

Biochemical parameters (AST and ALP) were determined calorimetrically in serum using specific kits (Biodiagnostic, Egypt) and following manufacturer procedures.

2.6.4 Preparation of tissue samples

Liver sections were homogenized (MPW-120 homogenizer, Med instruments, Poland) in PBS to obtain 20% homogenate and kept overnight at –80°C. The homogenates were centrifuged for 5 minutes at 5000 x g using a cooling centrifuge (Sigma and laborzentrifugen, 2k15, Germany). The supernatant was taken immediately, and used for oxidative stress biomarkers MDAGSH and CAT using chemical methods. SOD using commercial kits (Randox Laboratory, Crumlin, Ireland), apoptotic markers Caspase-3 (Casp-3), and inflammatory cytokines (TNF-α and IL-1β) using ELISA kits. All results are calculated 1mg total protein.

2.6.5 Determination of oxidative stress markers

Malondialdehyde (MDA), reduced glutathione (GSH), catalase (CAT), and superoxide dismutase (SOD) were determined according to the following methods [27-30] respectively.

2.6.5.1 Determination of MDA [27]

Malondialdehyde (MDA) a reactive aldehyde that is a measure of lipid peroxidation, was determined using a spectrophotometer. Mix 0.5 ml serum or organ homogenates, 0.5 ml physiological solution and 0.5 ml 25% trichloroacetic acid and centrifuged at 2,000 rpm for 20 min. A 1 ml of protein-free supernatant was mixed with 0.25 ml 0.5% thiobarbituric acid and heated at 95°C for 1 h. After cooling, the intensity of the pink color of the end fraction product was determined at 532 nm.

2.6.5.2 Determination of GSH [28]

Reduced glutathione (GSH) assessment is based on the reduction of 5,5-dithiobis-2-nitrobenzoic acid to produce a yellow compound. Tissue was deproteinized with 2 mol/l perchloric acid, centrifuged for 10 min. at 1000 ×g and the supernatant was neutralized with 2 mol/l potassium hydroxide. The reaction medium contained 100 mmol/l phosphate buffer (pH 7.2), 2 mmol/l nicotinamide dinucleotide phosphate acid, 0.2 U/ml glutathione reductase, 70 µmol/l 5,5-dithiobis (2-nitrobenzoic acid). To determine reduced glutathione, the supernatant was neutralized with 2 mol/l potassium hydroxide, reacted with 70 µmol/l 5,5-dithiobis (2-nitro benzoic acid), and read at 420 nm.

2.6.5.3 Determination of CAT activity [29]

Briefly, 10 μL of the sample was incubated with 100 μmol/mL of H_2O_2 in 0.05 mmol/L Tris-HCl buffer pH = 7 for 10 min. The reaction was terminated by rapidly adding 50 μL of 4% ammonium molybdate. The yellow complex of ammonium molybdate and H_2O_2 was measured at 410 nm. One unit of catalase activity was defined as the amount of enzyme required to decompose 1 μmol H_2O_2 per min.

2.6.5.4 Determination of SOD [30]

SOD activity was estimated on tissue homogenate using commercially available kits (Randox Laboratory, Crumlin, Ireland). Erythrocytes were hemolyzed by the addition of redistilled water and vigorous vortexing. Estimation of SOD activity was based on the generation of superoxide radicals produced by xanthine and xanthine oxidase, which react with 2-(4- iodophenyl)-3-(4-nitrophenol)-5-phenyltetrazolium chloride to form a red formazan dye. SOD activity is then determined by the degree of inhibition of this reaction.

2.6.6 Determination of apoptotic marker caspase-3 (Casp-3)

Caspase-3 was quantified in liver homogenate using a rat caspase-3 ELISA kit (Invitrogen, USA). The optical density (OD) of all samples at 450 nm was measured using a Spectramax (M2, Molecular Devices, USA).

2.6.7 Determination of inflammatory cytokines

TNF-α was assessed using a rat TNF-α kit (Invitrogen, USA) and (IL-1β) was determined using a rat (IL-1β) kit (R&D Systems, USA) in liver homogenates. The optical density (OD) used was 450 nm and measured using a Spectramax (M2, Molecular Devices, USA).

2.6.8 Histopathological examination

Different sections from the liver of normal control and other treated groups were fixed in 10% neutral formalin and routinely processed. Tissue sections of 5 µm thickness were stained with H&E for histopathological examinations. Additionally, the sections were stained with Masson trichrome stain for the demonstration of fibrous tissue and collagen fibers. For assessment of liver damage, the tissues were semi quantitively assessed according to Knodell, R.G. method [31], with some modifications. The assessment of hepatic damage was carried out in ten random low power fields per group.

2.6.9 Immunohistochemical analysis

Immunohistochemical staining of hepatic tissues for the demonstration of COX2 and NF-kβ was carried out according to the method of Abd Eldaim et al [32]. Briefly, the formalin-fixed hepatic and renal sections were deparaffinized, hydrated in alcohol solutions, and incubated in 3% H2O2. After that, the sections were incubated with rabbit polyclonal anti-COX2 (ab15191, Abcam, USA) and rabbit polyclonal anti- NF-kβ (ab16502 Abcam, USA) as primary antibodies. The immune reactivity was visualized by using diaminobenzidine (DAB; Sigma Chemical Co., USA). Immunohistochemical expression of COX2 and NF-kβ in the hepatic tissues was semi-quantitatively assessed in ten random high power fields (40X) according to the percentage of immune positive cells per high power fields as reported in a recent study [33].

2.7 Statistical Analysis

The effects of surfactant presence and surfactant type on particle size, PDI, and Zeta potential have been assessed. The variance analysis and interaction were conducted using Minitab software and SPSS software. Using Minitab tools, the desirability factors were analyzed.

Statistical analysis for the microbiological study was performed using the Statistical Package for Social Sciences (SPSS) software and Mstat-c Program. Descriptive statistics and ANOVA (One Way analysis) for the parametric variables were tested followed by LSD. All measurements are repeated three times (n=3) [34-35].

Hepatoprotective studies represented as mean ± SE. Statistical analysis was done by one-way analysis of variance (ANOVA) followed by Turkey test for confirmation and multiple comparisons.

3. RESULTS

3.1 Size, Zeta Potential, and Morphology of CTS

CTS was prepared using various techniques. Table 1 displays the average particle size (nm), zeta potential (mV), and polydispersity index (PDI) of the nanoparticles collected. Particle size results as presented in Table 1 & Fig1 showed that the mean nano-suspension diameter was between 54.3±20.8 and 1256±16.8 nm. Fig 1A showed that the nanoparticles prepared with L-α-lecithin (F1) displayed the largest particle size of 1256.3±16.8 nm followed by nanoparticles prepared with Tween 80 as a surfactant (F2) of 712.7±9.1 nm (Fig. 1B), followed by nanoparticles prepared with sodium alginate without any surfactant (F3), displaying the lowest particle size of 54±20.8 nm (Fig. 1C).

Table 1. Mean particle size, polydispersity index (PDI), and zeta potential of CTS of different formulas

Formula code	SAA type	HLB	PS (nm)	PDI	ZP (mV)
F1	L-α-lecithin	4	1256.3±16.8	0.274±0.09	24±1.2
F2	Tween 80	15	712.7±9.1	0.259±0.008	29.5±0.8
F3			54±20.8	0.553±0.06	30.8±1.1

HLB: hydrophilic-lipophilic balance, PS, particle size; PDI, polydispersity index; ZP, zeta potential. values are listed as mean ±SD

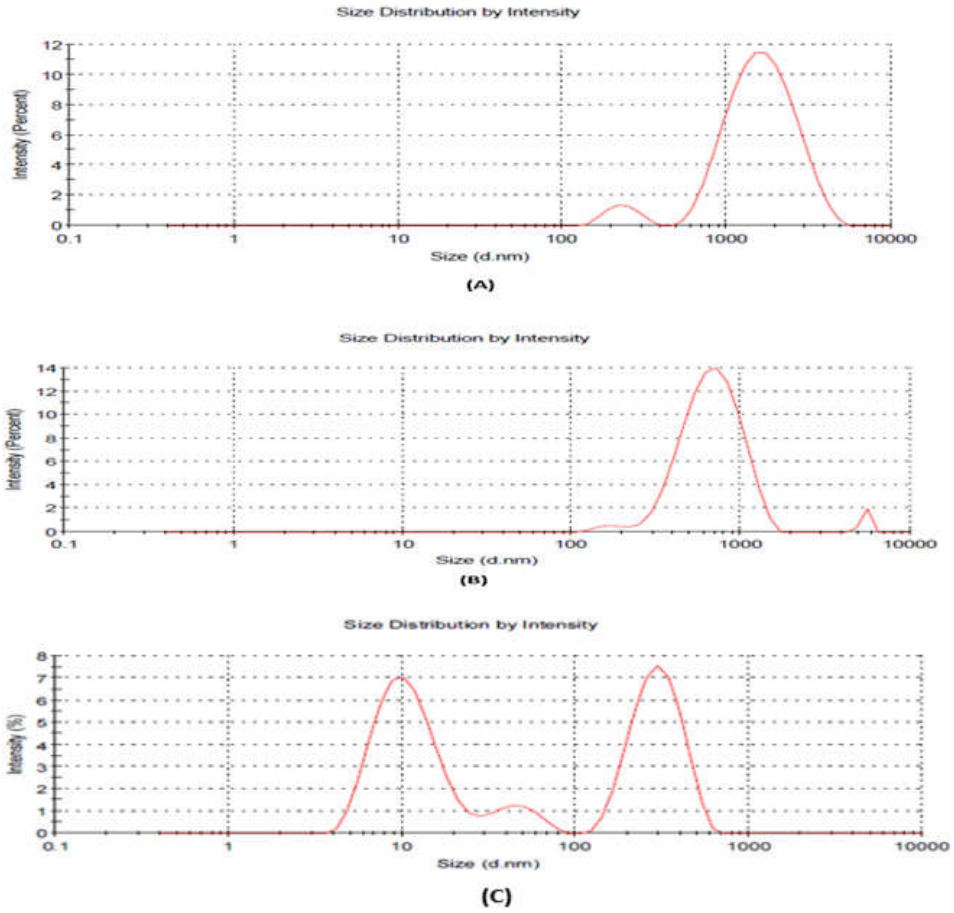

Fig. 1. The size distribution of CTS by diffraction light scattering in (nm). Fig A represent Formula 1(F1), Fig B represent Formula 2 (F2) and Fig C represent Formula 3 (F3)

Optical microscopy revealed that the particles were regular in shape with no assemblage for formula 3(F3) (Fig. 2C), then formula 1(F1) (Fig. 2A), and formula 2(F2) (Fig 2B).

For all formulations, the zeta potential ranged from 24±1.2 to 30.8±1.1. The zeta potential of Formula 3 (F3) was 30.8±1.1 mV (Fig. 3C), which is greater than that of 24±1.2 mV Formula 1 (F1) (Fig. 3A) and 29.5±0.8 mV Formula 2 (F2) (Fig. 3B). This high value of (F3) indicates a positively charged particle surface that emphasizes its good stability due to high electrostatic repulsion between positively charged particles, so that particle suspension stability is strongly affected. The higher positive charge of the nanoparticles also promotes in-vivo interaction, allowing the absorption of nanoparticles and their passage through the cell membrane channels of the bacteria, which are usually negatively charged.

Statistical analysis of the findings shown graphically in Fig. 4 (A) showed that the surfactant type had only an effect on particle size (significant $P<0.05$), where the use of L-α-lecithin (F1) resulted in a particle size greater than that of Tween 80 (F2), followed by nano-suspension prepared without surfactants (F3).

The surfactant type did not affect either PDI or zeta-potential as shown in Fig. 4(B) and Fig 4(C). Homogenous dispersion is shown by the PDI values for all samples. The optimal response was to decrease the particle size, PDI and increase the zeta-potential, based on the physicochemical properties of the nanoparticles, and the analysis of the effect of different surfactants and their effects on the desirability factor, as shown in Fig.5, using Minitab software, according to these conditions. The method of inotropic gelation was found to be appropriate in the preparation of chitosan alginate nanoparticles and formula 3

that had the smallest particle size, acceptable PDI and highest zeta-potential, ensuring stability and improving their passage through the cell membrane and ensuring that high residence time was chosen for further evaluation.

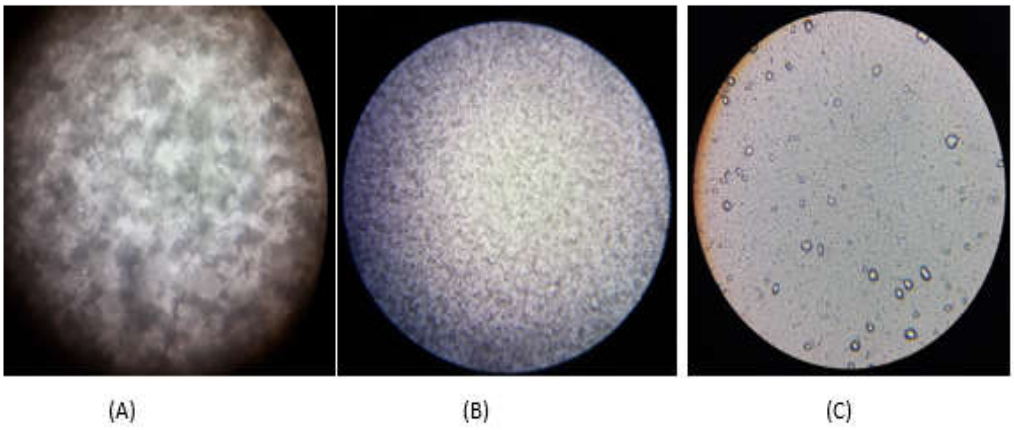

Fig. 2. CTS image by optical microscopy, (A) F1, (B) F2, (C) F3

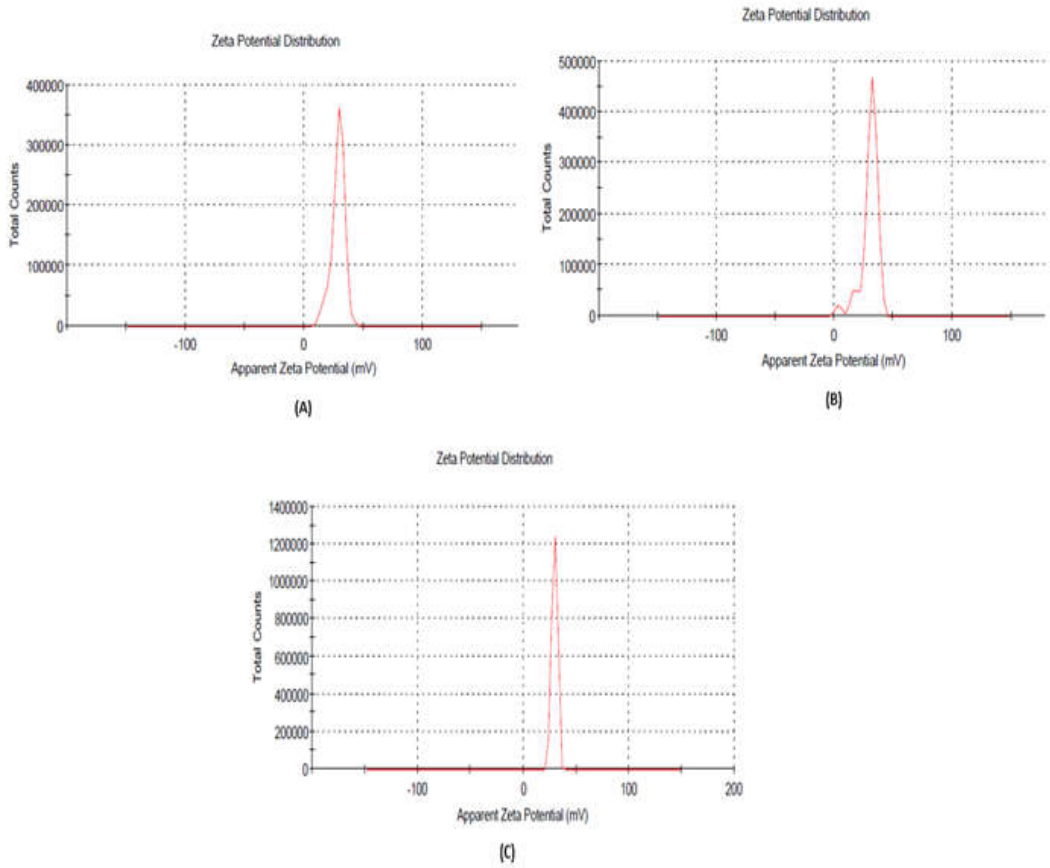

Fig. 3. Zeta potential distribution of CTS; Fig A represents Formula 1 (F1), Fig B represents Formula 2 (F2) and Fig C represents Formula 3 (F3)

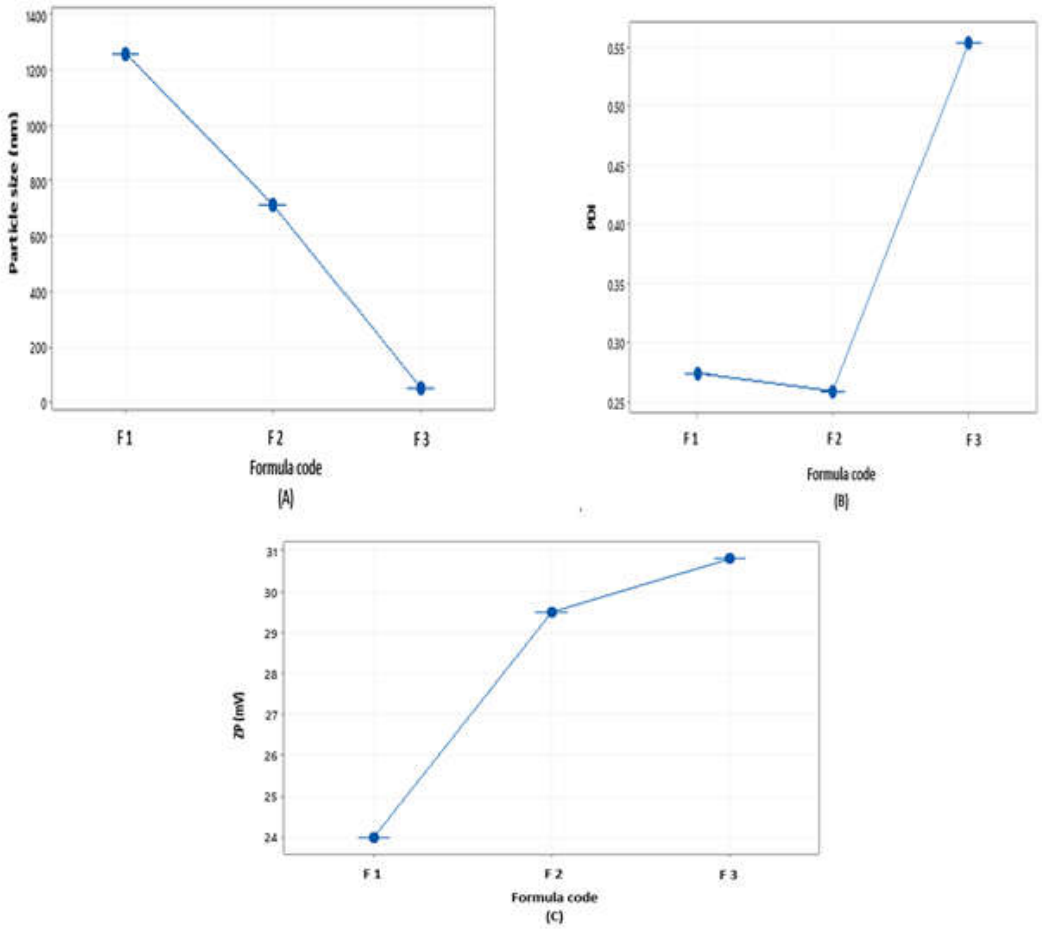

Fig. 4. The effect of Surfactant types on (A) particle size, (B) polydispersity index, (C) zeta potential of CTS

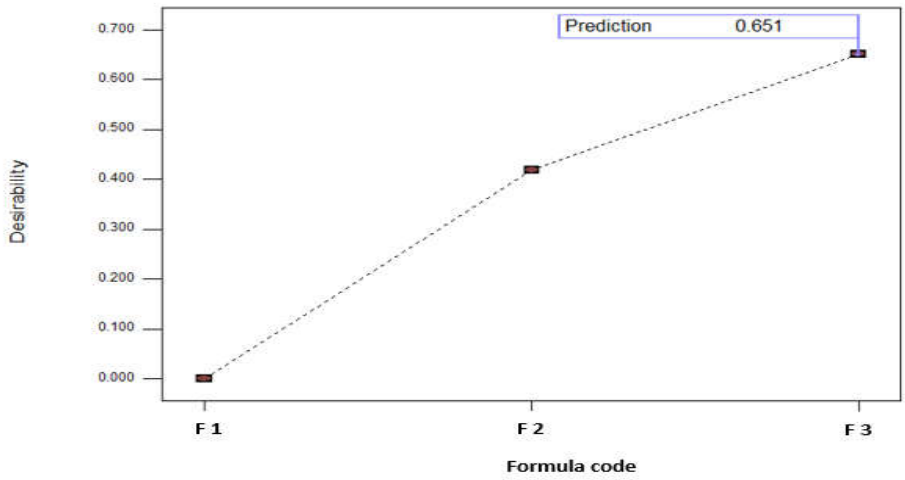

Fig. 5. The desirability factor of different formulas of chitosan nanoparticles

3.2 Antimicrobial Studies

3.2.1 Evaluation of Chitosan nanoparticles (CTS) antimicrobial activity

Screening the antibacterial effect of CTS against Gram-positive (*Bacillus subtilis*-ATCC6633, *Staphylococcus aureus* NRRLB-767,) and Gram-negative (*Escherichia coli* ATCC-25955, *Pseudomonas aeruginosa* -ATCC 101455) bacteria revealed the appearance of inhibition zones around all the tested microorganisms, while no inhibition zones were observed in the chitosan nano particle-free treatment (control) (Fig 6).

3.2.2 Measurements of inhibition zone diameter

The means of three measurements of inhibition zone diameter of CTS for *B.subtilis S.aureus, E. coli, Ps.aeruginosa* are summarized in Table 2 and represented in Fig 7. Results indicate a highly significant difference between the different chitosan nanoparticles (CTS) concentrations in their antibacterial effects against the pathogenic bacteria being studied. As CTS doses increased, the inhibition zones of all isolated bacteria grew larger. The highest inhibition zones were obtained with a high CTS dose (150 *μ*g/mL), and a decrease in concentration resulted in a decrease in the growth inhibition region. The lowest zones of inhibition by the CTS were found at a dose of 25 *μ*g/mL (α = 0.05).

3.2.3 Determination of minimum inhibitory concentration (MIC) and minimum bactericidal concentration (MBC)

The minimum inhibitory concentration (MIC) of CTS was quantitatively investigated using the turbidity method for the development of pathogenic organisms. The data presented in Table 3 showed that normal microbial growth inhibition behaviors were achieved; their antimicrobial activities were increased by increasing levels of the polymers studied. Statistical analysis of the results revealed a highly significant difference in the antibacterial effect of the various concentrations of CTS relative to the tested pathogenic bacteria, including those resistant to multiple antibiotics. MIC and MBC were ranged between 39.4 to 156.3 *μ*g/mL and 156.3 to 500 *μ*g/mL respectively at α = 0.01 level. *S. aureus* obtained the highest inhibitory effect at concentrations of 39.4 *μ*g/mL, but there is no significant difference between (156.5 *μ*g/mL, (312.5 *μ*g/mL) and (620 *μ*g/mL). The lowest inhibitory effect was obtained against *B. subtilis* at 156.3 *μ*g/mL, moreover, there is a significant difference between the results. Table 4 shows the MIC and MBC of CTS against the tested microorganisms. At 500, 156.5, 312.5, and 312.5 *μ*g/mL, CTS displayed full inhibition of *B. subtilis, S. aureus*, *E. coli,* and *Ps. aeruginosa*, respectively.

3.3 Hepatoprotective Studies

3.3.1 Measurement of liver biochemical parameters

Liver enzymes (AST and ALP) were measured in serum (Table 4). Results showed a significant elevation ($^{a}P \leq 0.05$) in AST and ALP concentrations in CCl_4 induced group (52.2±0.18 and 54.3±0.2 U/L respectively) when compared to the control -ve group (42.13±0.05 and 34.5±0.5 U/L respectively). Oral concurrent treatment of CCl_4 induced rats with CTS (10 mg/kg) showed no significant reduction ($^{b}P \leq 0.05$) in AST level (51.1±0.3U/L) as compared to CCl_4 induced, on the other hand, the same dose showed a significant reduction ($^{b}P \leq 0.05$) in ALP level (49.5±1.6U/L) when compared to CCl_4 induced group. Oral concurrent treatment of CCl_4 induced rats with CTS (20 mg/kg) showed a significant reduction ($^{b}P \leq 0.05$) in AST and ALP levels (47.03±0.4 and 42.2±0.5 U/L respectively) when compared to CCl_4 induced group. These results indicate that CTS (20 mg/kg) might have a regenerative effect on liver function by reducing AST and ALP biomarkers in the CCl_4 induced rat model.

3.3.2 Determination of oxidative stress parameters

Oxidative stress markers (MDA, GSH, CAT, and SOD) were determined in the liver homogenate. Results illustrated in Table (5) showed a significant increase ($^{a}P \leq 0.05$) in MDA and on contrary a significant decrease ($^{a}P \leq 0.05$) in (GSH, CAT, and SOD) concentrations in CCl_4 induced group (14.8±0.3 nmol/mg total protein, 0.35±0.015 nmol/mg total protein, 2.54±0.06 U/mg total protein, and 8.63±0.5U/mg total protein respectively). As compared to the control -ve group (5.7±0.05 nmol/mg total protein, 0.7±0.018 nmol/mg total protein, 4.6±0.04 U/mg total protein, and 17.46±0.4 U/mg total protein respectively), showing a percentage increase in MDA concentration to 156.07% and a percentage decrease in GSH, CAT and SOD concentrations to (50.46, 45.14 and 50.57 % respectively) in CCl_4 induced group as compared

to control -ve group. Oral concurrent treatment of CCl_4 induced rats with CTS (10 mg/kg) showed significant reduction ($^bP \leq 0.05$) in MDA level and a significant increase (bp ≤ 0.05) in GSH, CAT and SOD level (11.8±0.5 nmol/mg total protein, 0.56±0.015 nmol/mg total protein, 4.37±0.2 U/mg total protein, and 15.7±0.2 U/mg total protein respectively) as compared to CCl_4 induced. Oral concurrent treatment of CCl_4 induced rats with CTS (20 mg/kg) showed significant reduction ($^bP \leq 0.05$) in MDA level and a significant increase ($^bP \leq 0.05$) in GSH, CAT and SOD level (10.08±0.3 nmol/mg total protein, 0.6±0.01 nmol/mg total protein, 4.45±0.5 U/mg total protein, and 17.4±0.1 U/mg total protein respectively) as compared to CCl_4 induced. These results indicate that CTS (20 mg/kg) restored the CAT and SOD, which are enzymes capable of protecting cells from radical attack to their normal levels in the CCl_4 induced rat model.

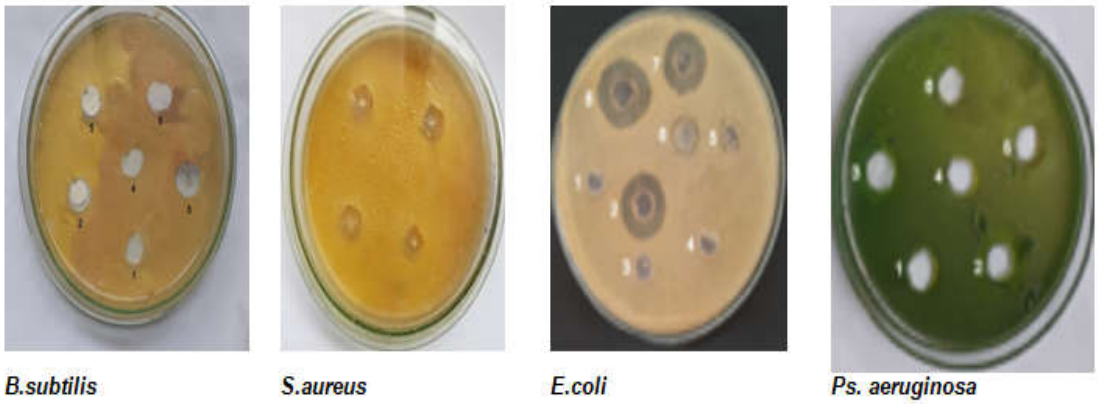

Fig. 6. Inhibition zone produced by CTS using agar well diffusion method

Table 2. Inhibition zones (mm) of bacterial growth on MH agar at different doses of CTS (*μ*g/mL) after 24-h incubation at 37 °C

Conc. (*μ*g/mL)	*B. subtilis*	*S. aureus*	*E. coli*	*Ps aeruginosa*
25	12.33^{c}±0.58	16.33^{d}±1.53	16.67^{c}±1.53	16.33^{b}±2.08
50	19.33^{b}±1.15	18.33^{cd}±1.53	21.67^{b}±1.53	16.67^{b}±2.08
75	18.67^{b}±1.15	19.67^{cd}±2.52	22.00^{b}±1.00	14.67^{b}±1.53
100	18.33^{b}±1.53	20.00^{bc}±2.00	23.00^{b}±1.73	16.33^{b}±1.15
125	19.67^{b}±0.58	23.33^{ab}±2.08	26.33^{a}±2.08	24.00^{a}±1.73
150	27.00^{a}±1.00	26.00^{a}±2.00	27.00^{a}±1.00	26.00^{a}±1.00

Values are represented as means ± standard deviation (SD) of at least three experiments (n = 3). Means with different superscripts are significant (α = 0.05) level and means without superscripts in common are not significant (α = 0.05)

Table 3. Effect of CTS different concentrations on the growth inhibition of *B. subtilis, S. aureus, E. coli*, and *Ps. aeruginosa* using Turbidity method at 620 nm

Chitosan conc *μ*g/mL	*B. subtilis*	*S. aureus*	*E. coli*	*Ps. aeruginosa*
0	1.440^{a}±0.027	1.400^{a}±0.010	1.360^{a}±0.061	1.300^{a}±0.090
4.9	1.363^{ab}±0.003	1.307^{b}±0.021	1.224^{b}±0.004	1.124^{b}±0.002
9.8	1.200^{b}±0.178	1.160^{c}±0.040	1.024^{c}±0.001	0.950^{c}±0.015
19.7	1.230^{b}±0.080	1.000^{d}±0.020	0.919^{d}±0.007	0.850^{d}±0.015
39.4	0.920^{c}±0.020	0.800^{e}±0.020	0.730^{e}±0.046	0.670^{e}±0.040
78.1	0.730^{d}±0.020	0.610^{f}±0.020	0.530^{f}±0.040	0.430^{f}±0.040
156.3	0.360^{e}±0.040	0.000^{g}±0.000	0.210^{g}±0.020	0.180^{g}±0.040
312.5	0.176^{f}±0.020	0.000^{g}±0.000	0.000^{h}±0.000	0.000^{h}±0.000
620	0.000^{g}±0.000	0.000^{g}±0.000	0.000^{h}±0.000	0.000^{h}±0.000

Values are means ± standard deviation (SD) of at least three experiments (n = 3. Means with different superscripts are significant (α = 0.01) and means without superscripts in common are not significant (α = 0.01)

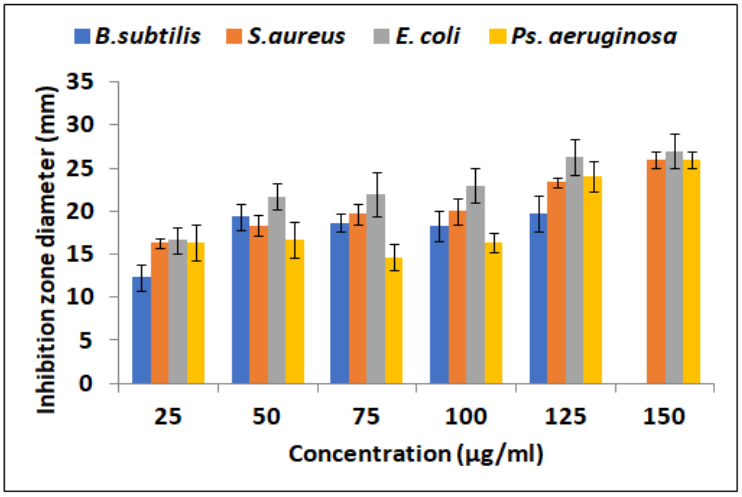

Fig. 7. Antibacterial activity of CTS against *B.subtilis* , *S.aureus, E. coli,* and *Ps. aeruginosa*
Values are represented as means ± standard deviation (SD) of at least three experiments (n = 3). Means with different superscripts within each column are significant (α = 0.05) level and means without superscripts in common are not significant (α = 0.05)

Table 4. Values of MIC and MBC (µg/mL) of CTS against tested microorganisms

Microorganisms	MIC concentration µg/mL	MBC concentration µg/mL
B. subtilis	156.3	500
S.aureus	39.4	156.3
E.coli	78.1	312.5
Ps. aeruginosa	78.1	312.5

Table 5. Effect of CTS (10 mg/kg and 20 mg/kg) on liver biochemical parameters in CCl_4 induced rat model of hepatotoxicity

Groups	AST (U/L)	ALP (U/L)
Control -ve	42.13±0.05	34.5±0.5
CCl_4 (1.5 ml/kg:i.p)	52.2±0.18^{a}	54.3±0.2^{a}
CTS (10 mg/kg)	51.1±0.3^{a}	49.5±1.6^{ab}
CTS (20 mg/kg)	47.03±0.4^{ab}	42.2±0.5^{ab}

Results were represented as (mean ± SE), (n = 10). Statistics were done using one-way (ANOVA) followed by Tukey's multiple comparison post hoc tests for confirmation. CCl_4, Carbon tetrachloride; CTS, Chitosan nanoparticles; AST, Aspartate aminotransferase; ALP, Alkaline Phosphatase; $^{a}P \leq 0.05$ represents a significant difference from the control negative group; $^{b}P \leq 0.05$ represents a significant difference from the CCl_4 group.

Table 6. Effect of CTS (10mg/kg and 20 mg/kg) on oxidative stress markers in CCl_4 induced rat model of hepatotoxicity

Groups	MDA(nmol/mg total protein)	GSH (nmol/mg total protein)	CAT (U/mg total protein)	SOD(U/mg total protein)
Control -ve	5.7±0.05	0.7±0.018	4.6±0.04	17.46±0.4
CCl_4 (1.5 ml/kg:i.p)	14.8±0.3^{a}	0.35±0.015^{a}	2.54±0.06^{a}	8.63±0.5^{a}
CTS (10 mg/kg)	11.8±0.5^{ab}	0.56±0.015^{ab}	4.37±0.2^{b}	15.7±0.2^{ab}
CTS (20 mg/kg)	10.08±0.3^{ab}	0.6±0.01^{ab}	4.45±0.5^{b}	17.4±0.1^{b}

Results were represented as (mean ± SE), (n = 10). Statistics were done using one-way (ANOVA) followed by Tukey's multiple comparison post hoc tests for confirmation. CCl_4, Carbon tetrachloride; CTS, Chitosan nanoparticles; MDA, Malondialdehyde; GSH, reduced glutathione; CAT, Catalase; SOD, Superoxide dismutase; $^{a}P \leq 0.05$ represents a significant difference from the control negative group; $^{b}P \leq 0.05$ represents a significant difference from the CCl_4 group

3.3.3 Determination of apoptotic marker caspase-3 (Casp-3)

The effect of CTS (10mg/kg) and (20mg/kg) on Casp-3 apoptotic marker was detected in the liver homogenate. Results illustrated in Fig. (8) showed a significant increase ($^{a}P \leq 0.05$) in Casp-3 level in CCl_4 induced group (2.33±0.04 ng/mg total protein) when compared to the control -ve group (1.4±0.1 ng/mg total protein). Oral treatment of CCl_4 induced rats with CTS (10mg/kg) and (20mg/kg) showed a significant reduction ($^{b}P \leq 0.05$) in Casp-3 level (1.95±0.1 and 1.81±0.06 ng/mg total protein respectively) as compared to CCl_4 induced group These results indicate that CTS (10mg/kg) and (20mg/kg) might improve the liver apoptosis induced by CCl_4.

3.3.4 Determination of inflammatory cytokines

Inflammatory cytokines (TNF-α and IL-1β) were determined in the liver homogenate and the results represented in Table (6) showed a significant increase ($^{a}P \leq 0.05$) in TNF-α and IL-1β concentrations in CCl_4 induced group (216.5±8.4 and 269.2±10.5 Pg/mg total protein respectively) as compared to the control -ve group (117.8±0.7 and 129.7±4.5 Pg/mg total protein respectively). Oral concurrent treatment of CCl_4 induced rats with CTS (10 mg/kg) showed a significant reduction ($^{b}P \leq 0.05$) in TNF-α Oral concurrent treatment of CCl_4 induced rats with CTS (10 mg/kg) showed a significant reduction ($^{b}P \leq 0.05$) in TNF-α and IL-1β levels (173.6±11.2 and 154.6±1.1 Pg/mg total protein respectively) as compared to CCl_4 induced group. (173.6±11.2 and 154.6±1.1 Pg/mg total protein respectively) as compared to CCl_4 induced group. Oral concurrent treatment of CCl_4 induced rats with CTS (20 mg/kg) showed a significant reduction ($^{b}P \leq 0.05$) in TNF-α and IL-1β levels (164.2±8.6 and 141.3±2.04 Pg/mg total protein respectively) as compared to CCl_4 induced group. These results indicate that CTS in a dose of (10 and 20 mg/kg) can exert their protective effect via inhibition of cytokine release.

3.4 Histopathological Studies

No histopathological lesions were demonstrated in the liver of the normal control group, in which normal hepatocytes with round vesicular nuclei (Fig 9a& 9b) and normal portal area (Fig 9c) were observed. Additionally, no inflammatory cellular infiltrates or fibroblastic proliferation was demonstrated in the portal area as confirmed by MTC stain (Fig 9d). On the contrary, remarkable histological alterations, varying from centrilobular hepatocellular necrosis, which is infiltrated by macrophages and lymphocytes to bridging necrosis associated with fibroblastic proliferation, were demonstrated in the CCl_4-treated group (Fig 9e & 9f). Portal areas were mildly infiltrated by mononuclear cells in addition to a hyperplastic proliferation of biliary epithelium (Fig 9g). Fibroblastic proliferation with collagen deposition extending into hepatic parenchyma was also demonstrated. The collagen fibers appeared blue in MTC-stained sections (Fig 9h). Marked attenuation of the histopathological lesions was recorded in CTS (10mg/kg) group, in which hepatocellular necrosis which is infiltrated by macrophages was confined to a focal area around the central vein and the remaining hepatocytes showed vacuolar degeneration (Fig 9i & 9j). Mild inflammatory cellular infiltrates were demonstrated in the portal area (Fig 9k). Additionally, in MTC-stained sections, no collagen deposition was demonstrated in this group (Fig 9l). Pronounced amelioration, with a significant decrease of the pathologic lesion scoring, was demonstrated in CTS (20mg/kg), in which hepatocellular necrosis was demonstrated in few hepatocytes surrounding the central vein, with no evidence of bridging necrosis (Fig. 9m & 9n). Minimal mononuclear cells were demonstrated in the portal area (Fig. 9o) without fibroblastic proliferation as confirmed in MTC-stained sections (Fig 10p).

Table 7. Effect of CTS (10mg/kg and 20 mg/kg) on inflammatory cytokines in CCl_4 induced rat model of hepatotoxicity

Groups	TNF-α (Pg/mg total protein)	IL-1β (Pg/mg total protein)
Control -ve	117.8±0.7	129.7±4.5
CCl_4 (1.5 ml/kg:i.p)	216.5±8.4^{a}	269.2±10.5^{a}
CTS (10 mg/kg)	173.6±11.2^{ab}	154.6±1.1^{ab}
CTS (20 mg/kg)	164.2±8.6^{ab}	141.3±2.04^{b}

Results were represented as (mean ± SE), (n = 10). Statistics were done using one-way (ANOVA) followed by Tukey's multiple comparison post hoc tests for confirmation. CCl_4, Carbon tetrachloride; CTS, Chitosan nanoparticles; TNF-α, Tumor necrosis factor; IL-1β, Interleukin-1β; $^{a}P \leq 0.05$ represents a significant difference from the control negative group; $^{b}P \leq 0.05$ represents a significant difference from the CCl_4 group

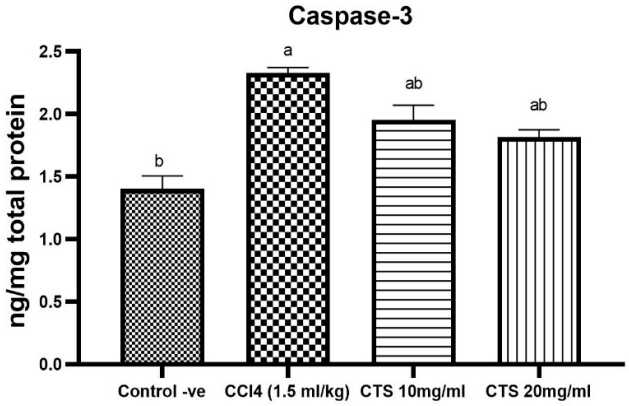

Fig. 8. Effect of CTS (10mg/kg and 20 mg/kg) on the apoptotic marker (Casp-3) in CCl_4 induced rat model of hepatotoxicity

All data are presented as mean ± SE (n=10), [a]P value of ≤ 0.05 was assumed to denote statistical significance. aP ≤ 0.05 Compared to the control -ve, [b]P ≤ 0.05 vs CCl_4 group. CCl_4, Carbon tetrachloride; CTS, Chitosan nanoparticles

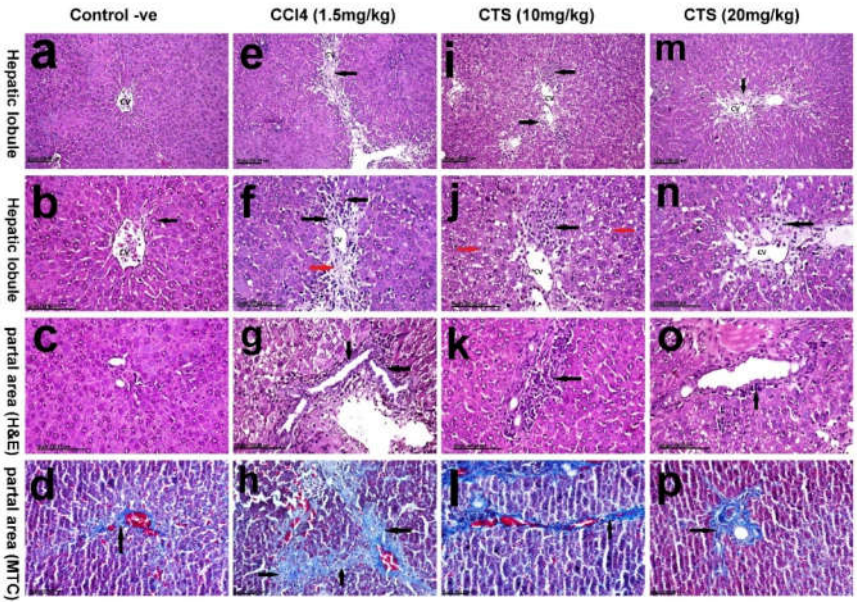

Fig. 9. Liver of , (a,b,c,d) normal control rats showing normal hepatocytes with round vesicular nuclei (arrow) (a & b) and normal portal area (c) with normal weakly stained fibrous tissue in the portal area (arrow) (d), (e,f,g,h) CCl_4-treated rats showing bridging necrosis (black arrows) associated with fibroblastic proliferation (red arrow) (e & f), hyperplastic proliferation of biliary epithelium (arrows) (g) and intense blue stained collagen fibers extending into hepatic parenchyma (arrows) (h), (I,j,k,l) CTS (10mg/kg) group showing focal hepatocellular necrosis infiltrated by macrophages (black arrows) and vacuolar degeneration of the surrounding hepatocytes (red arrows) (I & j), mild inflammatory cellular infiltrates in the portal area (arrow) (k) and normal blue-stained fibrous tissue in portal area (arrow) (l), (m,n,o,p) CTS (20mg/kg) group showing few necrotic hepatocytes surrounding the central vein with no evidence of bridging necrosis (arrows) (m & n), minimal mononuclear cells infiltrating the portal area (arrow) (o) and normal blue-stained fibrous tissue in portal area (arrow) (Stain: H&E for all photomicrograph except for d, h,l and p, the stain is MTC; Scale bar=100 µm)

3.5 Immunohistochemical Studies

3.5.1 COX2 immunohistochemical expression

No COX2 expression was demonstrated in the liver of the normal control group (Fig 10a). In contrast, a significant increase of COX2 expression was recorded in the liver of the CCl_4-treated group, which showed an increased percentage of positively stained cells with strong cytoplasmic staining of hepatocytes and renal tubular epithelium (Fig 10b). Additionally, COX2 expression was also demonstrated in the infiltrating inflammatory cells. Treatment with CTS showed a significant decrease of COX2 expression in the liver in a dose corresponding manner, with a significant difference between them (Fig 10c & 10d, respectively).

3.5.2 NF-kβ immunohistochemical expression

The Liver of the normal control group showed normal weak cytoplasmic staining of hepatocytes without nuclear staining (Fig 11a). On the contrary, a significant increase of NF-kβ expression was recorded in the liver of the CCl_4-treated group, in which nuclear translocation with strong nuclear staining was demonstrated (Fig 11b). On the other side, a significant decrease of NF-kβ expression with a decreased percentage of positive cells with positive nuclear staining has been recorded in the liver of the CTS (10 mg/kg) group (Fig 11c). A Significant difference was recorded in CTS (20mg/kg) group, in which nuclear staining was demonstrated in the infiltrating inflammatory cells (Fig 11d).

4. DISCUSSION

Nanotechnology has grown in popularity because of the unique properties of nanoparticles, which allow new applications. Using different techniques, CTS has been prepared, formula 3 showed the best fitted to nanoparticles. Results showed that the nanoparticles prepared with L-α-lecithin (F1) displayed particle size of 1256.3 ± 16.8 nm, 24 ± 1.2 mV for zeta potential ,and 0.274 ± 0.09 for PDI, this may be attributed to the different ionic nature of L-α-lecithin (anionic) and chitosan that has a cationic nature that leads to the high attraction between them, the electrostatic linkage between the protonated amine group of chitosan at acidic pH with the strong negatively charged amine group of L- α-lecithin may be the reason for increasing particle size and lowering the zeta potential [36-38].

This result was diverse from those of Alkholief [21] in particle size 157.67 ± 2.65nm, while the zeta-potential and PDI were comparable to 28.144± 0.84 mV and 0.271 ± 0.008 respectively.

The nanoparticles prepared using Tween 80 as a surfactant (F2) showed particle size 712.7± 9.1 nm, zeta-potential 29.5 ± 0.8 mV, and PDI 0.259 ± 0.008. This may be due to the formation of hydrogen bonds between oxyethylene moieties of Tween 80 and hydroxyl groups of chitosan [39].

This result was close to the particle size 554.2 ± 40.46 nm of Sukmawati *et al.* [40], while PDI was 0.44 ± 0.12.

The least particle size 54±20.8 nm, zeta-potential 30.8±1.1 mV, and PDI 0.553±0.06 were shown by the nanoparticles prepared by ionotropic gelation with sodium alginate without any surfactant (F3), the higher charge of the nanoparticles of chitosan (F3) may be attributed to the interactions between alginate as a core and chitosan undergoing polyelectrolyte complexion. The amine groups on chitosan in aqueous solutions were positively charged at a pH ranging from 4 to 5.5. In addition, alginate was negatively charged in a neutral pH solution where the carboxylate groups were charged. Approximately chitosan amino groups interacted with carboxylate alginate groups in aqueous solutions at pH 5 to form a polyelectrolyte complex, which gave an opalescent suspension with a positive zeta potential of approximately 30.8±1.1 mV suggesting high nano-suspension stability without particle aggregation [41].

This result was close to that of Thai *et al.* [42] whose particle size ranged from 50-80 nm, although it is different from the result shown by Katuwavila [20], whose particle size was 100 ± 28 nm, while the zeta-potential and PDI were comparable to 36 ± 3 mV, 0.414 ± 0.065 respectively so that the optimum formula F3 is the one prepared without any surfactant using ionotropic gelation technique. This study documented a method of preparing chitosan nanoparticles based on cationic chitosan inotropic gelation and polyelectrolyte complex formation between two polymers, this method is simple, rapid, and straightforward.

Emerging antibiotic resistance calls for new therapeutic approaches to be established. This has forced scientists to look for eco-friendly antimicrobial agents that show beneficial effects against pathogenic microorganisms resistant to

antibiotics. Several studies have established the antibacterial activity of chitosan nanoparticles as a precise and sensitive technique to monitor a variety of bacterial, fungal, and viral diseases [43-46]. Regularly, antimicrobial agents and disinfection have been researched for prospective application in a variety of hospital settings and labs [47-48], to sterilize medical surroundings and equipment and prevent the transmission of infectious diseases, which has resulted in thousands of deaths due to hospital-acquired infections [49].

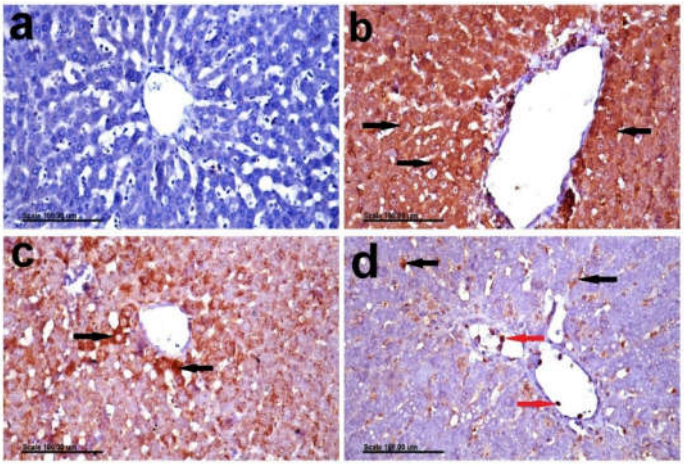

Fig. 10. photomicrograph showing COX2 immunohistochemical expression in the liver of normal control rats showing no COX2 expression the liver (a), CCl_4-treated rats showing the increased percentage of positively stained cells with strong cytoplasmic staining of hepatocytes (arrows) (b), CTS (10mg/kg) group showing the decreased percentage of positively stained hepatocytes (arrows) (c) and CTS (20mg/kg) group showing few COX2 positively stained cells in the hepatocytes and inflammatory cells (arrows) (d) (COX2 immunohistochemical staining; Scale bar=100µm)

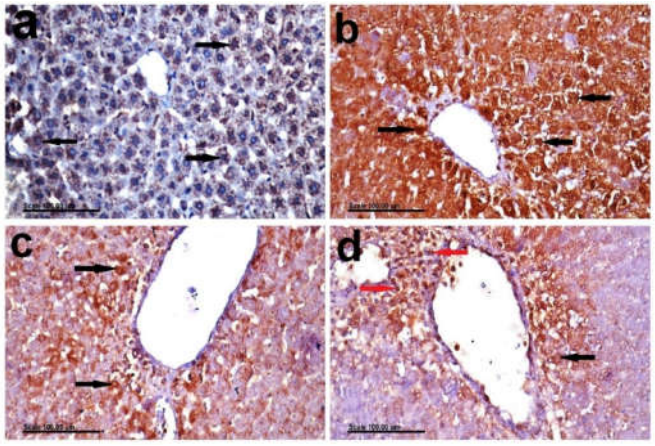

Fig. 11. photomicrograph showing NF-kβ immunohistochemical expression in the liver of normal control rats showing normal weak cytoplasmic staining of hepatocytes (arrows) (a), CCl_4-treated rats showing a significant increase of NF-kβ expression with strong nuclear staining of hepatocytes (arrows) (b), CTS (10mg/kg) group showing a significant decrease of NF-kβ expression with a decreased percentage of positive cells with positive nuclear staining in the hepatocytes (arrow) (c) and CTS (20mg/kg) group showing nuclear staining in the infiltrating inflammatory cells and most hepatocytes (arrows) (d). (NF-kβ immunohistochemical staining; Scale bar=100µm)

CTS was investigated for antibacterial activity against four pathogenic bacteria: *B.subtilis, S.aureus, E.coli*, and *Ps. aeruginosa*. The results of this investigation back up the role of chitosan nanoparticles in previous strain inhibition, demonstrating that the inhibition zone was directly proportional to chitosan nanoparticle concentrations, resulting in bacteriostatic or bactericidal inhibition. According to the literature, chitosan possesses antimicrobial activity against many Gram-negative [50-51] and Gram-positive bacteria [52-53]. Minimum inhibitory concentration (MIC) and minimum bactericidal concentration (MBC) were used to quantify the antibacterial activity of chitosan nanoparticles against the tested organisms. The CTS MIC and MBC values ranged from 39.4 to 156.3 *µ*g/mL and 156.3 to 500 *µ*g/mL, respectively. Higher CTS MIC's were reported by Younes *et* al. [53], who found that their range for *K. pneumoniae, E. coil, S. typhi*, *S. aureus*, and *M. luteus* was 0.01-1.0 mg/mL. Benhabiles *et al*. [51] indicated that the range of MIC for *E. coli Ps. aeruginosa* and *B. cereus* was 0.1–0.5mg/mL. *S.aureus* obtained the highest inhibitory effect with MIC and MBC of 39.4 *µ*g/mL and 156.3 *µ*g/mL, respectively .*E. coli* and *Ps. aeruginosa* had the best concentration, 312.5 *µ*g/mL, which provided maximum inhibition and zero OD (MBC), while MIC was 78.1 *µ*g/mL for both. for both. This could be because a peptidoglycan-layered exterior gram-positive bacterial membrane is insufficient to allow bacteria to thrust [6]. In this regard, Jeon *et al*. [54] revealed that chitosan was more effective against Gram-positive than Gram-negative bacteria. In comparison with our findings, Omura *et al*. stated that the chitosan preparations tested were reasonably resistant to *B. subtilis*, *P. aeruginosa*, and *E. coli* [55]. CTS was found to have stronger antibacterial effects against Gram-negative bacteria *E. coli* and *Ps. aeruginosa* (78.1 *µ*g/mL) than Gram-positive bacteria *B. subtilis* (156.3 *µ*g/mL) in the current investigation. As a consequence of this inference, Gram-negative bacteria possess an outer membrane containing lipopolysaccharide, which provides a hydrophilic surface for the bacterium, and peptidoglycan and teichoic acid are part of the cell wall of Gram-positive bacteria. This negative charge of Gram-negative bacteria was greater on the cell surface, these results in more chitosan adsorbed and higher inhibitory activity on Gram-negative bacteria than that on Gram-positive bacteria. In a separate article, Allan and Hardwiger stated that chitosan had a wide range of activities and a high degree of inhibition against both Gram-positive and Gram-negative bacteria [56]. Furthermore, Schnurch [57] documented the bacteriostatic and bactericidal activity of chitosan. This is because chitosan appears to disrupt the bacterial cell's outer membrane, penetrates the cell, and collapses materials inside the cell (Mohy-Eldin *et al*.,) [58]. Although the exact mechanism of chitosan's bactericidal action is unknown, its antibacterial activity in an acidic environment may be related to its polycationic structure, which is induced by the protonation of -NH2 on the D-glucosamine repeat unit's C-2 position. Chitosan, which is positively charged, can bind to the negatively charged bacterial cell surface and disrupt normal membrane functions, such as allowing intracellular component leakage or preventing nutrient transfer into cells [25]. Chitosan is a potential, naturally occurring preservative that can protect a variety of materials from microbial attack, albeit at low pH values. Because of their high antibacterial activity and acceptable biocompatibilities, chitosan nanoparticles are expected to be widely used as antimicrobial agents in medicine.

CCl_4 is used as a source of reactive oxygen species intracellular. The hepatotoxicity induced by CCl_4 is thought to be dependent on the partial pressure of the reactive oxygen species inside the liver cells, where the low partial pressure results in the production of CCl3 and CHCl2 free radicals while the high partial pressure is the leading cause for the release of CCl3-OO free radicals which in turn causes lipid peroxidation, that damages the hepatocellular membrane and steatosis that leads finally to cell apoptosis [59]. The apoptosis was also assessed in our study by measuring the apoptotic factor Casp-3 which showed a significant increase as a response to CCl_4 in rats as compared to the control -ve group. Our current findings were in line with these previous studies, where we reported that the CCl_4 caused an impairment in the natural antioxidant defense mechanism, presented by a significant increase in MDA level and on the other hand a severe decrease in GSH as well as a significant decrease in CAT and SOD. CAT and SOD are considered the first-line defense strategy in response to superoxide anion radical (aO2) which is perpetually generated via mitochondrial energy production pathway (MEPP) aiming to protect cells from radical attack and thus maintain cell membrane integrity and cellular viability [60]. This oxidative stress is usually followed by proinflammatory cytokine release *viz* TNF-α and interleukins. TNF-α and IL-1β are produced inside Kupffer cells as a

response to the oxidative stress induced by CCl_4 which in turn will exacerbate inflammation and end in cell apoptosis [61]. It has been reported previously that GSH deficiency also occurs as a result of the susceptibility of liver cells to TNF-α [62]. In parallel to these studies, our results showed that the group injected with CCl_4 only showed a significant increase in TNF-α, IL-1β, and COX2 as compared to the control -ve group. These results indicated hepatic cell injury represented by elevation in liver biomarkers as AST and ALP as a result of CCl_4 induced hepatotoxicity as these markers are released in serum as a result of liver cells degeneration, increased cell membrane permeability, and liver cell necrosis [63]. The same results were reported by Dutta et al., [62]. The oxidative stress, inflammatory and apoptotic effect of CCl_4 had been ameliorated by oral administration of CTS nanoparticles in two doses (10 and 20 mg/kg) concurrently with an injection of CCl_4 for 15 consecutive days. Both doses showed a significant decrease in MDA level as well as a significant elevation of GSH, CAT, and SOD in liver homogenate. CTS nanoparticles (10 and 20 mg/kg) also showed a significant decrease in the apoptotic biomarker; Casp-3 as well as a significant decrease in proinflammatory cytokines release (TNF-α and IL-1β). A previous study was done to investigate the effect of CTS against non-alcoholic fatty liver disease (NAFLD) induced in rats and results showed amelioration of TNF-α and IL-6 levels and thus exerting an anti-inflammatory effect [64]. All these findings indicated an improvement in liver function that was also confirmed by the amelioration of AST and ALP in sera. A previous study showed that administration of CTS reversed the elevated liver AST and ALP induced by CCl_4 and the researchers attributed this effect due to the inhibition of hepatic satellite cells (HSCs) [65]. All our findings were confirmed with histopathological studies that showed a prominent ameliorative effect of CTS in a dosed manner against the hepatocyte damage that occurred as a result of CCl_4 toxicity. Therefore, the study is a strong demonstration of the applicability of CTS as an efficient antimicrobial and hepatoprotective agent.

5. CONCLUSION

CTS was prepared by the ionotropic gelation method. The physicochemical characteristics of nanoparticles were analyzed using Zetasizer and optical microscopy. The development of new therapeutic strategies is being forced by antibiotic resistance. As a result, the antibacterial activity of CTS against multidrug-resistant pathogens such as *Bacillus subtilis, Staphylococcus aureus, Escherichia coli*, and *Pseudomonas aeruginosa* was assessed using the minimum inhibitory concentration process (MIC). The chitosan nanoparticles used in this analysis emphasize CTS' therapeutic ability as an antimicrobial against the pathogens examined. Concurrent treatment of CTS in both dose levels (10 and 20 mg/kg) with CCl_4 for 14 successive days succeeded to reduce the CCl_4 induced hepatotoxicity via ameliorating the liver enzymes in serum (AST & ALP), oxidative stress (MDA, GSH, CAT, and SOD), apoptotic (Caspase-3) and the inflammatory (TNF-α and IL-1β) elevated biomarkers in liver tissues. Additionally, the histopathological and immunohistochemical studies showed a prominent regenerative effect on liver cells. Accordingly, we can attribute the significant hepatoprotective impact of chitosan nanoparticles to its antioxidant and anti-inflammatory effects.

CONSENT

It is not applicable.

ETHICAL APPROVAL

The experimental protocol was approved by the Ethics and Animal Care Committee of the National Research Centre (NRC-MREC) and following the recommendations of the National Institutes of Health Guide for Care and Use of Laboratory Animals (NIH Publications No. 8023, revised 1978).

COMPETING INTERESTS

Authors have declared that no competing interests exist.

REFERENCES

1. Rouget C. Des substances amylacées dans les tissus des animaux, spécialement des Articulés (chitine). Comptes rendus Hebd des séances l ' Académie des Sci. 1859;48:792–5.
2. Pochanavanich P, Suntornsuk W. Fungal chitosan production and its characterization. Lett Appl Microbiol. 2002;35(1):17–21.
3. Greven H, Kaya M, Baran T. The presence of α-chitin in Tardigrada with comments on

chitin in the Ecdysozoa. Zoologischer Anzeiger-A Journal of Comparative Zoology. 2016;264:11-6.
4. Kaya M, Baublys V, Šatkauskienė I, Akyuz B, Bulut E, Tubelytė V. First chitin extraction from Plumatella repens (Bryozoa) with comparison to chitins of insect and fungal origin. International journal of biological macromolecules. 2015;79:126-32.
5. Malmiri HJ, Jahanian MAG, Berenjian A. Potential applications of chitosan nanoparticles as novel support in enzyme immobilization. Am J Biochem Biotechnol. 2012;8(4):203–19.
6. Morin-Crini N, Lichtfouse E, Torri G, Crini G. Fundamentals and Applications of Chitosan. In 2019.
7. Tao Y, Qian LH, Xie J. Effect of chitosan on membrane permeability and cell morphology of Pseudomonas aeruginosa and Staphyloccocus aureus. Carbohydr Polym. 2011;86(2):969–74.
8. Sahayaraj K, Rajesh S. Bionanoparticles: Synthesis and antimicrobial applications. Sci against Microb Pathog; 2011.
9. Kaya M, Akyuz B, Bulut E, Sargin I, Eroglu F, Tan G. Chitosan nanofiber production from Drosophila by electrospinning. International journal of biological macromolecules. 2016;92:49-55.
10. Gupta AK, Naregalkar RR, Vaidya VD, Gupta M. Recent advances on surface engineering of magnetic iron oxide nanoparticles and their biomedical applications. Nanomedicine. 2007;2:23–39.
11. Muzzarelli R, Tarsi R, Filippini O, Giovanetti E, Biagini G, Varaldo PE. Antimicrobial properties of N-carboxybutyl chitosan. Antimicrob Agents Chemother. 1990;34(10):2019–23.
12. Rabea EI, Badawy MET, Stevens C V., Smagghe G, Steurbaut W. Chitosan as antimicrobial agent: Applications and mode of action. Vol. 4, Biomacromolecules. 2003;1457–65.
13. Young DH, Köhle H, Kauss H. Effect of Chitosan on Membrane Permeability of Suspension-Cultured Glycine max and Phaseolus vulgaris Cells . Plant Physiol. 1982;70(5):1449–54.
14. Shahidi F, Arachchi JKV, Jeon YJ. Food applications of chitin and chitosans. Vol. 10, Trends in Food Science and Technology. 1999;37–51.
15. No HK, Young Park N, Ho Lee S, Meyers SP. Antibacterial activity of chitosans and chitosan oligomers with different molecular weights. Int J Food Microbiol. 2002;74(1–2):65–72.
16. Kong M, Chen XG, Xing K, Park HJ. Antimicrobial properties of chitosan and mode of action: A state of the art review. Vol. 144, International Journal of Food Microbiology. 2010;51–63.
17. Slavin YN, Asnis J, Häfeli UO, Bach H. Metal nanoparticles: Understanding the mechanisms behind antibacterial activity. Journal of Nanobiotechnology; 2017.
18. Taamalli A, Feriani A, Lozano-Sanchez J, Ghazouani L, El Mufti A, Allagui MS, et al. Potential hepatoprotective activity of super critical carbon dioxide olive leaf extraCTS against CCl_4-induced liver damage. Foods. 2020;9(6):804.
19. Ma JQ, Ding J, Zhang L, Liu CM. Ursolic acid proteCTS mouse liver against CCl_4-induced oxidative stress and inflammation by the MAPK/NF-κB pathway. Environ Toxicol Pharmacol. 2014;37(3):975–83.
20. Katuwavila NP, Perera ADLC, Samarakoon SR, Soysa P, Karunaratne V, Amaratunga GAJ, et al. Chitosan-Alginate Nanoparticle System Efficiently Delivers Doxorubicin to MCF-7 Cells. J Nanomater. 2016;2016:2016.
21. Alkholief M. Optimization of Lecithin-Chitosan nanoparticles for simultaneous encapsulation of doxorubicin and piperine. J Drug Deliv Sci Technol. 2019;52:204–14.
22. Pathak L, Amrutanand T, Agrawal Y. Alginate-chitosan coated lecithin core shell nanoparticles for curcumin: Effect of surface charge on release properties and biological activities. Indian J Pharm Educ Res. 2017;51(2):270–9.
23. Catchpole CR. Bailey and Sott's Diagnostic Microbiology, 9th edition: EJ Baron, LR Peterson and S. M. Finegold. 1994. ISBN 0-8016-6987-1. Mosby-Year Book, Inc., St Louis. Pp. 958. 39.95. J Med Microbiol. 1995;42(4):308–308.
24. Wiegand I, Hilpert K, Hancock REW. Agar and broth dilution methods to determine the minimal inhibitory concentration (MIC) of antimicrobial substances. Nat Protoc; 2008.
25. Abdeltwab WM, Abdelaliem YF, Metry WA, Eldeghedy M. Antimicrobial effect of chitosan and nano-chitosan against some pathogens and spoilage microorganisms.

Journal of Advanced Laboratory Research in Biology. 2019;10(1):8-15.
26. Hassan S, Elbakry M, Mangoura S, Omar Z. Evaluation of the effect of Gallic acid against carbon tetrachloride-induced liver injury in albino rats: histological, immunohistochemical and biochemical study. J Med Histol. 2017;1(2):202–15.
27. Tüközan N, Erdamar H, Seven I. Measurement of Total Malondialdehyde in Plasma and Tissues by High-Performance Liquid Chromatography and Thiobarbituric Acid Assay. Fırat Tıp Derg. 2006;11(2):88–92.
28. Tipple TE, Rogers LK. Methods for the determination of plasma or tissue glutathione levels. Vol. 889, Methods in Molecular Biology. 2012;315–324.
29. Aebi H. [13] Catalase in vitro. Methods Enzym. 1984;105:121–6.
30. Nishikimi M, Appaji Rao N, Yagi K. The occurrence of superoxide anion in the reaction of reduced phenazine methosulfate and molecular oxygen. Biochem Biophys Res Commun. 1972;46(2):849–54.
31. Knodell RG, Ishak KG, Black WC, Chen TS, Craig R, Kaplowitz N, et al. Formulation and application of a numerical scoring system for assessing histological activity in asymptomatic chronic active hepatitis. Hepatology. 1981;1(5):431–5.
32. Abd Eldaim MAA, Abd El Latif AS, Hassan A, El-Borai NB. Ginseng attenuates fipronil-induced hepatorenal toxicity via its antioxidant, anti-apoptotic, and anti-inflammatory activities in rats. Environ Sci Pollut Res. 2020;27(36):45008–17.
33. Asaad GF, Hassan A, Mostafa RE. Anti-oxidant impact of Lisinopril and Enalapril against acute kidney injury induced by doxorubicin in male Wistar rats: involvement of kidney injury molecule-1. Heliyon. 2021;7(1).
34. Duncan DB. Multiple Range and Multiple F Tests. Biometrics. 1955;11(1):1.
35. Snedecor GW, Cochran WG. Statistical Methods. 8th Edition, Iowa State University Press, Ames. - References - Scientific Research Publishing;1989.
36. Gerelli Y, Barbieri S, Di Bari MT, Deriu A, Cantu L, Brocca P, Sonvico F, Colombo P, May R, Motta S. Structure of self-organized multilayer nanoparticles for drug delivery. Langmuir. 2008;24(20):11378-84.
37. Şenyiğit T, Sonvico F, Barbieri S, Özer Ö, Santi P, Colombo P. Lecithin/chitosan nanoparticles of clobetasol-17-propionate capable of accumulation in pig skin. Journal of Controlled Release. 2010;142(3):368-73.
38. Sonvico F, Cagnani A, Rossi A, Motta S, Di Bari MT, Cavatorta F, Alonso MJ, Deriu A, Colombo P. Formation of self-organized nanoparticles by lecithin/chitosan ionic interaction. International journal of pharmaceutics. 2006;324(1):67-73.
39. Luque-Alcaraz AG, Lizardi-Mendoza J, Goycoolea FM, Higuera-Ciapara I, Argüelles-Monal W. Preparation of chitosan nanoparticles by nanoprecipitation and their ability as a drug nanocarrier. RSC advances. 2016;6(64):59250-6.
40. Sukmawati A, Utami W, Yuliani R, Da'I M, Nafarin A. Effect of tween 80 on nanoparticle preparation of modified chitosan for targeted delivery of combination doxorubicin and curcumin analogue. In: IOP Conference Series: Materials Science and Engineering;2018.
41. Sæther HV, Holme HK, Maurstad G, Smidsrød O, Stokke BT. Polyelectrolyte complex formation using alginate and chitosan. Carbohydrate Polymers. 2008;74(4):813-21.
42. Thai H, Thuy Nguyen C, Thi Thach L, Thi Tran M, Duc Mai H, Thi Thu Nguyen T, et al. Characterization of chitosan/alginate/lovastatin nanoparticles and investigation of their toxic effects in vitro and in vivo. Sci Rep. 2020;10(1).
43. Shaalan M, Saleh M, El-Mahdy M, El-Matbouli M. Recent progress in applications of nanoparticles in fish medicine: A review. Vol. 12, Nanomedicine: Nanotechnology, Biology, and Medicine. 2016;701–10.
44. Akmaz S, Dilaver Adgüzel E, Yasar M, Erguven O. The effect of ag content of the chitosan-silver nanoparticle composite material on the structure and antibacterial activity. Adv Mater Sci Eng. 2013;2013.
45. Chirkov SN. The antiviral activity of chitosan (review). Vol. 38, Applied Biochemistry and Microbiology. 2002;1–8.
46. Feng QL, Wu J, Chen GQ, Cui FZ, Kim TN, Kim JO. A mechanistic study of the antibacterial effect of silver ions on Escherichia coli and Staphylococcus aureus. J Biomed Mater Res;2000.
47. Mohamed AA, Ali SI, Darwesh OM, El-Hallouty SM, Sameeh MY. Chemical compositions, potential cytotoxic and

antimicrobial activities of nitraria retusa methanolic extract sub-fractions. Int J Toxicol Pharmacol Res. 2015;7(4):204–12.
48. Hosseinnejad M, Jafari SM. Evaluation of different factors affecting antimicrobial properties of chitosan. Vol. 85, International Journal of Biological Macromolecules. 2016;467–75.
49. Yılmaz Atay H, Çelik E. Investigations of antibacterial activity of chitosan in the polymeric composite coatings. Prog Org Coatings. 2017;102:194–200.
50. Andres Y, Giraud L, Gerente C, Le Cloirec P. Antibacterial effects of Chitosan powder: Mechanisms of action. Environ Technol. 2007;28(12):1357–63.
51. Benhabiles MS, Salah R, Lounici H, Drouiche N, Goosen MFA, Mameri N. Antibacterial activity of chitin, chitosan and its oligomers prepared from shrimp shell waste. Food Hydrocoll. 2012;29(1):48–56.
52. Van Toan N, Thi Hanh T, Vo Minh Thien P. Antibacterial Activity of Chitosan on Some Common Food Contaminating Microbes. Open Biomater J. 2013;4:1–5.
53. Younes I, Hajji S, Frachet V, Rinaudo M, Jellouli K, Nasri M. Chitin extraction from shrimp shell using enzymatic treatment. Antitumor, antioxidant and antimicrobial activities of chitosan. Int J Biol Macromol. 2014;69:489–98.
54. Jeon YJ, Park PJ, Kim SK. Antimicrobial effect of chitooligosaccharides produced by bioreactor. Carbohydr Polym. 2001;44(1):71–6.
55. Omura Y, Shigemoto M, Akiyama T, Saimoto H, Shigemasa Y, Nakamura I, et al. Antimicrobial activity of chitosan with different degrees of acetylation and molecular weights. Biocontrol Sci. 2003;8(1):25–30.
56. Allan CR, Hadwiger LA. The fungicidal effect of chitosan on fungi of varying cell wall composition. Exp Mycol. 1979;3(3):285–7.
57. Bernkop-Schnürch A. Chitosan and its derivatives: Potential excipients for peroral peptide delivery systems. Vol. 194, International Journal of Pharmaceutics. 2000;1–13.
58. Mohy Eldin MS, Soliman EA, Hashem AI, Tamer TM. Antibacterial activity of chitosan chemically modified with new technique. Trends Biomater Artif Organs. 2008;22(3):125–37.
59. Zhang Q, Wu G, Guo S, Liu Y, Liu Z. Effects of tristetraprolin on doxorubicin (adriamycin)-induced experimental kidney injury through inhibiting IL-13/STAT6 signal pathway. Am J Transl Res. 2020;12(4):1203–21.
60. Feng Y, Wang N, Ye X, Li H, Feng Y, Cheung F, et al. Hepatoprotective effect and its possible mechanism of Coptidis rhizoma aqueous extract on carbon tetrachloride-induced chronic liver hepatotoxicity in rats. J Ethnopharmacol. 2011;138(3):683–90.
61. Ighodaro OM, Akinloye OA. First line defence antioxidants-superoxide dismutase (SOD), catalase (CAT) and glutathione peroxidase (GPX): Their fundamental role in the entire antioxidant defence grid. Alexandria J Med. 2018;54(4):287–93.
62. Dutta S, Chakraborty AK, Dey P, Kar P, Guha P, Sen S, et al. Amelioration of CCl_4 induced liver injury in swiss albino mice by antioxidant rich leaf extract of Croton bonplandianus Baill. PLoS One. 2018;13(4):e0196411.
63. Matsumaru K, Ji C, Kaplowitz N. Mechanisms for sensitization to TNF-α induced apoptosis by acute glutathione depletion in murine hepatocytes. Hepatology. 2003;37(6):1425–34.
64. AboZaid O, AbdEl-hamid O, Atwa S. Hypolipidemic and anti-inflammatory effect of chitosan in experimental induced non - alcoholic fatty liver disease in rats. Benha Vet Med J. 2015;28(1):155–65.
65. Zhong-Feng W, Mao-Yu W, De-Hai Y, Zhao Y, Hong-Mei X, Zhong S, et al. Therapeutic effect of chitosan on CCl_4-induced hepatic fibrosis in rats. Mol Med Rep. 2018;18(3):3211–8.

Peer-review history:
The peer review history for this paper can be accessed here:
https://www.sdiarticle4.com/review-history/73066